CALCULATING THE EFFECT OF DUAL-AXIS SCANNER ROTATIONS AND SURFACE ORIENTATION ON SCAN PROFILES

Conor Cahalane, Conor P. McElhinney and Tim McCarthy

National Centre for Geocomputation (NCG),
National University of Ireland Maynooth (NUIM),
Maynooth, Co. Kildare, Ireland,
conor.cahalane.2010@nuim.ie, conormce@cs.nuim.ie, tim.mccarthy@nuim.ie
http://ncg.nuim.ie/

KEY WORDS: Mobile, Laser scanning, Resolution, Surface, Performance, Standards

ABSTRACT:

The large volumes of point cloud data collected by a Mobile Mapping System(MMS) equipped with a laser scanner have attracted the attention of the research community, primarily towards developing automated algorithms to help when processing this data. This has resulted in insufficient attention being paid to quantifying the capabilities of these systems, and due to the relative youth of this technology there is no concrete understanding of the point density that different hardware configurations and operating parameters will exhibit on objects at specific distances. Obtaining the required point density for a project impacts on survey time, processing time, data storage and is the underlying limit of automated algorithms. Lack of understanding of these systems makes defining point density in project specifications a complicated process. We are in the process of developing a method for determining the quantitative resolution of point clouds collected by a MMS with respect to known objects at specified distances. We have previously demonstrated the effect that scanner orientation in one axis, scanner configuration and scanner operating speed have on scan profiles. We have also focused on the effect on scan profiles of the combined vertical and horizontal rotations of the scanner (dual-axis rotations) and also incorporated point spacing for planar surfaces at different scanner mirror speeds, pulse repetition rates and field of view as a function of range into our model. The subject of this paper is to investigate the effect that a dual-axis scanner rotation has on profile spacing and to design a theoretical system to calculate the angular change on profiles exhibited on horizontal and vertical surfaces for different system configurations. The second goal of the research presented in this paper is to include in our calculations a method for incorporating surfaces that are not parallel to the direction of travel or that are not perfectly vertical, such as walls facing away from the road or sloped surfaces. Profile angle impacts on profile spacing and is a major factor in calculating point density on arbitrary objects, such as road signs, poles or buildings, all important features in asset management surveys. A number of tests were designed to investigate these issues and the results show that these tests have justified our methods, but it has been made apparent that vehicle dynamics play a larger role than anticipated.

1 INTRODUCTION

The focus of the research community to date has largely been on developing automated or semi-automated algorithms for processing the large point clouds captured by modern terrestrial or mobile mapping systems (Becker and Haala, 2009, Hammoudi et al., 2009, Pu and Vosselman, 2007). However, other than accuracy tests on specific systems (Barber et al., 2008, Haala et al., 2008) little research exists assessing the performance of generic mobile mapping systems. Further research in this area is important as one of the underlying questions facing research groups working with extraction algorithms is what point density to expect for objects at different ranges. For example, work by (Kukko et al., 2009) and (Lehtomäki et al., 2010) require a minimum number of profiles on post objects for them to be detected. Circular objects need a minimum number of points on each profile to recognise a circular shape. Each algorithm performs differently, and from (Kaartinen et al., 2005) we can see that point density directly impacts on the accuracy of the resulting extracted model. Mobile mapping systems (MMS) are new to the market, and to date there has been no concerted effort to assess their combined capabilities. This paper will focus solely on laser based systems.

One of the fundamental decisions when assembling a laser based mobile mapping system is the location and orientation of the scanner on the vehicle. Although there have been tests investigating the best scanner configuration to minimise occlusions (Yoo et al., 2009), there does not appear to have been research carried out to find the optimal location for a single scanner (i.e. rear, side, front) that will provide the highest point density. Our system is a single scanner system, so we hope to provide a definitive view of its capabilities which we anticipate will then be of use to systems operating more than one scanner. The orientation of the scanner is also of importance. Scan lines cannot be perpendicular to the direction of travel or they will miss objects whose sides are also perpendicular to it. A horizontal rotation of the scanner solves this problem, and a vertical rotation deals with structures above the vehicle which would otherwise be missed, such as overhead road signs or bridge faces. We hope to be able to define what the optimum orientation is when surveying for particular features.

When safe to do so, mobile mapping systems are capable of operating at highway speeds. However, point density decreases as vehicle velocity increases and this necessitates multiple passes to ensure a dense point cloud (multiple passes are also employed to ensure all sides of an object are captured) that will meet project specifications. To ensure a high point density, projects have been carried out at low speed (Goulette et al., 2006, Graefe, 2007), which in a commercial situation would impact on the productivity of a MMS. It is our hope that when completed our work will allow us define the maximum speed for specific scanner configurations that will provide a required point density, and also define the minimum number of passes required. This should help to minimise survey time, processing time and also the file size resulting from each survey.

To date there has been some interesting work in the area of point density acquired by mobile mapping systems. (Kukko et al.,

2007) and (Hesse and Kutterer, 2007) have qualitatively measured profile spacing at certain mirror speeds and vehicle velocities. We hope to improve on this by providing a generic formula which will work for any mirror speed, vehicle velocity and importantly, will incorporate scanner orientation into the system. (Hofmann and Brenner, 2009) have included in their work on theoretic point density some interesting results on the effect change in vehicle direction and velocity has on scan lines. A recent study (Riveiro et al., 2011) testing the metrology specifications of terrestrial laser scanners (including resolution) shows how current this issue is, and as TLS is a more mature technology than MMS the justification for beginning this work should be apparent. We have previously (Cahalane et al., 2010a) designed a method for calculating the profile spacing for a MMS on planar, orthogonal surfaces with a single axis scanner rotation, varying mirror frequencies and vehicle velocity. We have also qualitatively defined (Cahalane et al., 2010b) the angular change caused by dual axis scanner rotations on perfectly vertical planar surfaces and a quantitative method for calculating point spacing on profiles for different systems on planar surfaces at different ranges.

In the following section we will look at mobile mapping systems in general and the platform we have developed at StratAG, followed in Section 3 by the theory behind our current work on calculating profile angles. Section 4 will display the results of our test data, and finally in Section 5, our conclusions.

2 MOBILE MAPPING AND XP1

A MMS enables high density spatial data to be collected along route networks. These data can then be utilised in a number of ways, such as route safety audits, road authorities GIS, infrastructure surveys and change detection for national mapping agencies. Combining high accuracy GNSS/INS, LiDAR and imaging sensors on-board a moving platform enable surveys to be carried out rapidly and in a cost effective manner(Haala et al., 2008). Land based MMS compliment existing ground based survey and aerial surveying activities in a number of ways. Large scale detail such as road sign detail or detailed infrastructure condition can be recorded. Additionally, extensive ground control is not required and these systems can capture features that are sometimes obscured from aerial platforms(Barber et al., 2008).

The multi-disciplinary research group StratAG, established to research advanced geotechnologies at NUI Maynooth have completed design and development of a multi-purpose, state of the art, land based Mobile Mapping System (XP-1). The primary components of the XP-1 are an IXSEA LANDINS GPS/INS, a Riegl VQ-250 300KHz laser scanner and an imaging system consisting of 6 progressive-scan cameras. Imaging sensors include a FLIR thermal (un-cooled) SC-660 camera and an innovative 5-CCD multi-spectral camera capable of sensing across blue, green, red and two infra-red bandwidths. We will now detail the theory behind calculating the angle of laser profiles for a MMS.

3 LASER SCANNER PROFILES

When a laser scanner operating a rotating mirror is mounted on a moving platform, the forward motion of that platform creates individual scan lines (or scan profiles) for each mirror rotation. Rotations of the scanner in the horizontal or vertical plane change the angle of scan profiles on horizontal and vertical surfaces, altering profile spacing and ultimately point density. In this section we will describe our method for calculating the angular effect that dual axis scanner rotations and angled surfaces have on profiles. This is an important factor in quantitatively calculating the profile spacing and hence the point density for arbitrary objects. We will now explore the effect that the combination of horizontal and vertical rotations of the scanner have on profile angles.

3.1 Surface normals

As we are designing a method to calculate point density that will be system independent, the only information available to us when calculating the angle of profiles on surfaces is the orientation of those surfaces and the orientation of the scanner. The method we have designed for calculating this utilises surface normals, rotation matrices and geometrical formulae. A surface normal is a vector perpendicular to a planar surface. We can represent this by a 1×3 matrix. For example, in the coordinate system displayed in Figure 1 the surface normal of the vertical wall (N_{wall}) parallel to the direction of travel is directly to the right along the x axis, [1, 0, 0] and the road surface normal (N_{ground}) is vertically upwards, along the z axis, [0, 0, 1].

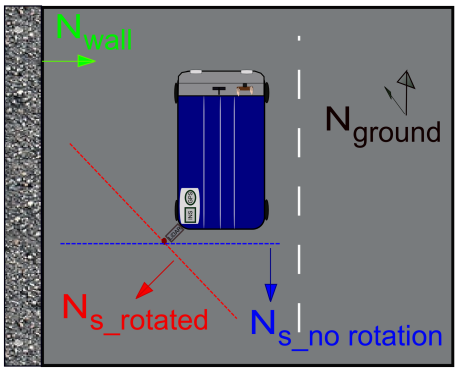

Figure 1: Surface Normals

The surface normal of a rotated scanplane must be found by applying the vertical and horizontal rotations of the scanner to the rotation matrices,

$$R_x(\theta) = \begin{bmatrix} 1 & 0 & 0 \\ 0 & \cos\theta & -\sin\theta \\ 0 & \sin\theta & \cos\theta \end{bmatrix} \quad (1)$$

$$R_y(\theta) = \begin{bmatrix} \cos\theta & 0 & \sin\theta \\ 0 & 1 & 0 \\ -\sin\theta & 0 & \cos\theta \end{bmatrix} \quad (2)$$

$$R_z(\theta) = \begin{bmatrix} \cos\theta & -\sin\theta & 0 \\ \sin\theta & \cos\theta & 0 \\ 0 & 0 & 1 \end{bmatrix} \quad (3)$$

creating a rotation matrix, and then applying this rotation matrix to the scanplane. The scanner is at the rear of the vehicle facing backwards, so the initial scanplane surface normal is [0, -1, 0].

To illustrate this process, when a $45^\circ \times 45^\circ$ rotation of the scanner in the horizontal and vertical planes is implemented, the scan normal before any rotation of the scanner is multiplied by a series of rotation matrices, depending on which plane it is rotated around. For a horizontal and vertical rotation it is rotated around $R_z(\theta)$ and $R_x(\theta)$ respectively. Figure 2(a) illustrates a horizontal and Figure 2(b) a vertical rotation of the scanner.

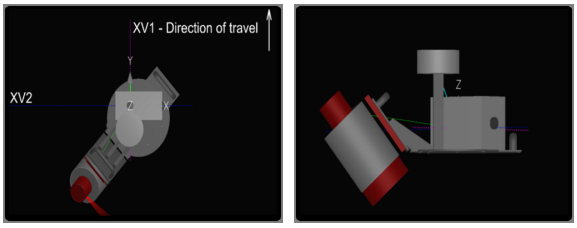

(a) (b)

Figure 2: Laser scanner rotations - horizontal(a) vertical(b)

The rotation matrix for a dual axis scanner rotation is found by multiplying the three rotation matrices

$$(N_{s-rotated}) = R_x(\gamma)R_y(\beta)R_z(\alpha), \tag{4}$$

where γ, β and α are the vertical, axial and horizontal rotation angles respectively. Applying this to the initial scanplane gives an amended surface normal for a $45^\circ \times 45^\circ$ horizontal and vertical rotation of the scanner of [-0.5, -0.5, 0.7071]. This process of applying rotation matrices to planes is also how we will calculate the surface normals of rotated or angled surfaces when exploring their effect on profile angles in Section 3.3.

3.2 Dual axis rotation theory

Our previous work has identified the effect that dual axis rotations of the scanner have on profile angles and has also provided a method for qualitatively calculating this for a selection of scanner rotations (Cahalane et al., 2010b). We will now present our method for quantitatively calculating this for any combination of scanner rotations.

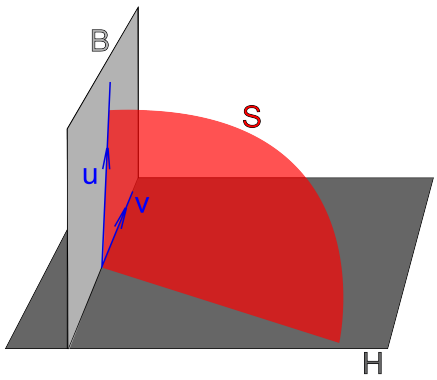

Figure 3: Scan planes

Figure 3 displays three planes. H represents the horizontal plane (the ground), B the vertical plane (a building face) and S the rotated scanplane. Each of these planes have a surface normal vector which is perpendicular to their surface. For ease of reference, the vertical normal becomes b, the scanplane normal becomes s, and the ground normal becomes h, differing from Figure 1. This can be illustrated for the scanplane by

$$'x.s = 0' \quad S = \{x|x \perp scan\ normal\}, \tag{5}$$

for the horizontal plane by

$$'x.h = 0' \quad H = \{x|x \perp horizontal\ normal\}, \tag{6}$$

and for the building plane by

$$'x.b = 0' \quad B = \{x|x \perp building\ normal\}. \tag{7}$$

As shown in Figure 3, the scanplane intersects the building plane and creates a vector u

$$\{\lambda u|\lambda \varepsilon R\} = S \cap B = \{x|x \perp s,\ x \perp b\}, \tag{8}$$

whereas the horizontal and building planes intersect and form vector v

$$\{\lambda v|\lambda \varepsilon R\} = H \cap B = \{x|x \perp h,\ x \perp b\}. \tag{9}$$

The angle formed between vectors u and v is the profile angle, the goal of this study. Vector u is perpendicular to the scan vector, s and also to the building vector, b

$$u \perp s,\ u \perp b,\ \|u\| = 1. \tag{10}$$

It can be calculated where $\times$ is the cross product with

$$u = \frac{s \times b}{|s \times b|}. \tag{11}$$

Vector v is perpendicular to the horizontal vector and also to the building vector

$$v \perp h,\ v \perp b,\ \|v\| = 1. \tag{12}$$

It can be calculated with

$$v = \frac{h \times b}{|h \times b|}. \tag{13}$$

The spherical angle ($\sphericalangle$) between two vectors can be found using

$$\cos \sphericalangle(u, v) = u.v, \tag{14}$$

and as vectors u and v are also a product of two vectors, this is then expanded, where $\cdot$ is the dot product to

$$\cos \sphericalangle(u, v) = \frac{(s \times b) \cdot (h \times b)}{|s \times b||h \times b|}. \tag{15}$$

This process can be repeated for any combination of scanner rotations using an amended scanplane surface normal. We will now expand this process to include angled or rotated surfaces.

3.3 Angled Surface Theory

To date, our work has focused on vertical or horizontal surfaces that were perfectly planar and parallel to one face of the MMS. To move one step closer to modelling a real world system, we will now incorporate angled or sloped surfaces. Although any surface can be rotated around three axes (R_x, R_y or R_z) only two of

the axes will impact on the profile angle. These two axes vary depending on which surface is being rotated, the horizontal or the vertical. For instance, if a vertical surface is rotated by R_x it will not change the profile angle. In our system we are introducing surface normals to assist in calculating profile angle. As described in Section 3.1, we will apply the rotation matrices to the the standard surface normals for horizontal and vertical surfaces. We will rotate the vertical surface horizontally by using the rotation matrix R_z (to represent surfaces converging with/diverging from the direction of travel), and angle it (to represent sloped surfaces such as roof tops) by using the rotation matrix R_y. These amended surface normals can then be substituted into Equation 15, and the profile angle for an arbitrary scanner rotation and surface rotation can be found in this way. We will now illustrate the methods we have identified for experimentally validating this system using three datasets.

4 RESULTS AND DISCUSSION

We hope to demonstrate the capabilities of our prediction system by using three datasets for verification. One is a theoretical dataset, designed in a computer aided drawing (CAD) environment (Figure 4(a)) , the second is a real world point cloud captured by our XP1 MMS of a test route designed specifically for this research (Figure 4(b)) at NUIM and the third is a real world point cloud captured by our XP1 MMS of existing features, such as walls and buildings captured during a project in the U.K. For each dataset we identified a number of suitable areas for tests and a series of sample measurements were taken at each location. For each dataset, the profile angle was manually measured.

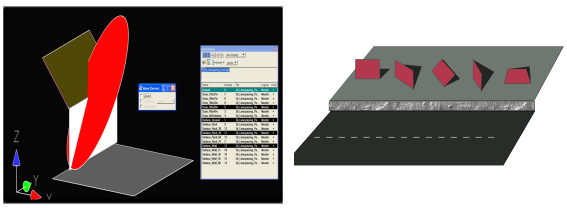

(a) CAD Dataset (b) Test route

Figure 4: CAD Dataset and manufactured test route.

4.1 Dataset 1 - CAD Environment

For our initial tests, we created a number of planes representing different surfaces and different scanner rotations in a CAD environment (Figure 4(a)). Dataset 1 consists of fifty tests, constituting five horizontal surface rotations and five vertical surface rotations for five different dual axis scanner rotations. We were then able to manually measure the profile angle on each surface for each dual axis scanner rotation in the CAD environment. A further benefit to using the CAD environment for our initial tests was that each profile would be identical unless the surface or scanplane were changed, implying that any error present would be entirely due to the manual measurement process. To give an idea of the magnitude of this effect, the variance was calculated for five measurements of the same profile, on the same surface. Measurements in the CAD environment displayed a variance (σ^2) of 0.01. This is entirely due to human error, and therefore can also be expected in the other datasets. The difference between the predicted profile angle and the measured profile angle of this test and the two remaining tests have been summarised in Table 1. Dataset 1 displays the lowest errors of the three, with a minimum error of 0°, a mean error of 0.1° and a maximum error of 0.48°, verifying our theoretical system. A real world test could now be applied.

Table 1: Dataset Errors - dec. degrees

No.	max error	min error	mean error
1	0.48	0	0.1
2	3.65	1.15	2.23
3	5.92	0.27	3.00

4.2 Dataset 2 - Manufactured Test Site

After the successful completion of the CAD tests which verified our theoretical model, the next stage of our testing required us to compare real world point cloud data captured by our XP1 mobile mapping system of a test route designed specifically for this project. The subject of this paper is to investigate the effect of dual axis rotations and rotated or sloped structures on profile angles. However, as we cannot vary the rotations of our scanner due to a rigid mounting, we had to vary the rotation of the surfaces. The test route consisted of a series of large, planar rectangular targets positioned at regular intervals along a roadside. Twelve targets were placed along the direction of travel. The targets were parallel, rotated horizontally, angled vertically and also a combination of horizontal and vertical. A portion of the test route is conceptualised in Figure 4(b).

Certain targets were placed at different ranges to test the robustness of the system (not visualised in Figure 4(b)). The parallel targets were chosen for exploring the dual axis rotation effect introduced in Section 3.2 while the horizontally rotated and vertically sloped targets were chosen for identifying the effect of angled surfaces on profile angles as introduced in Section 3.3. For each of the twelve targets, a sample of five measurements were taken of the profile angle, and because we were dealing with angles the circular mean was used

$$\bar{\alpha} \quad = \arctan 2(\frac{1}{n} \cdot \sum_{j=1}^{n} \sin \alpha_j, \frac{1}{n} \cdot \sum_{j=1}^{n} \cos \alpha_j), \qquad (16)$$

where α_j is a vector of size, n containing the measurements. As the angles were so similar, and not near the $0^\circ, 360^\circ$ point this was not strictly necessary and showed no deviation from the standard mean, however, as this system is being designed for general systems this may not always be the case.

As has been identified in Section 4 the manual measurement process will introduce differences between individual measurements. Another issue involved when dealing with real world point clouds, is accurately estimating the orientation of the surface in the horizontal and vertical axes. This too was a manual process, which presumably will also contribute errors. Initial investigations into the results identified variation in vehicle roll, pitch and yaw impacting on the measurements, causing deviation from our predicted values, something that it had been hoped use of a test site would avoid. The results for the predicted and measured profile angles on vertical and horizontal surfaces of different orientations are displayed in Figure 5 and the errors have been summarised in Table 1. In this dataset our predictions are consistently greater than the measured in each case, caused by some external factor affecting the predicted values. Upon examining the navigation files for the test route it was noted that the MMS was experiencing a constant roll and pitch during the tests, an effect that would have to be explored further. Although the errors were higher for Dataset 2 than in the previous test, we were now operating our system in a real world environment from a moving platform, and so this was not unexpected. These errors also seem to be systematic, something which we hope to be able to identify and then

incorporate into our system. Calculating the variance of the sample measurements for these twelve targets gave a maximum σ^2 of 0.1, a mean of 0.02 and a minimum of 0.01. The higher variance when compared to the CAD environment is likely due to manual measurement error and changes in pitch, roll and yaw. As these were specially chosen targets, we could be sure they were perfectly planar. This would not be the case when selecting real world features in the next set of tests. We then examined profile angles on existing real world features in Dataset 3.

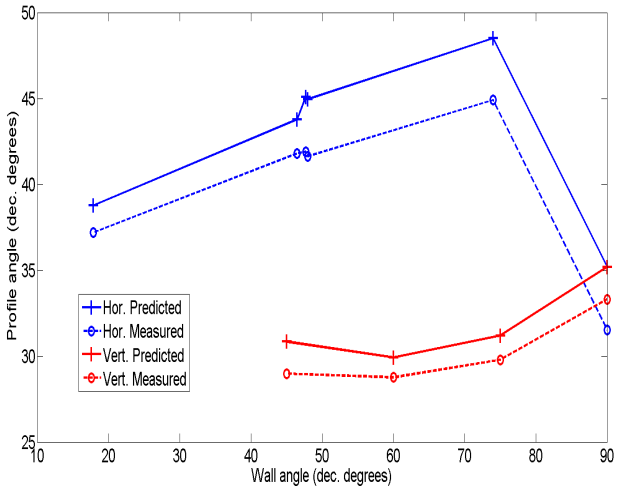

Figure 5: Profile angles for targets along test route - Dataset 2

4.3 Dataset 3 - Existing Features

After the completion of the CAD tests and also the use of data from the test route which in turn verified our theoretical model and then assessed it experimentally we could proceed with the final set of tests. This step required us to compare real world point cloud data captured by our XP1 mobile mapping system of real world features and see how our predictions for angular change performed against this test data. We chose man made features such as walls and building faces, and were able to use the 3D point cloud to measure the horizontal and vertical angles of these features. Using software designed by researchers at the NCG (Lewis et al., 2010), we were able to identify and extract areas of interest quickly from very large survey files. Figure 6 displays the results of the predicted profile angles and the measured profile angles for seventeen different surfaces, and Table 1 summarises these errors. Ten manual measurements of the profile angle were taken on each surface. It was hoped that this increase in the number of measurements per surface would help identify and eliminate surfaces that were non planar, and therefore improve the reliability of the results. As most surfaces had a vertical and horizontal rotation of some form, they were plotted together. This is why the predicted curve is not as smooth as might be expected, because certain features were not perfectly vertical. Calculating the variance of the sample measurements on each of these seventeen surfaces gave a maximum σ^2 of 0.16, a mean of 0.07 and a minimum of 0.02. Aside from the previously identified sources of error, this may also be due to the surfaces not being perfectly planar, or the surface occurring at a point where the vehicle heading is varying (i.e. the road curving).

Figure 6 exhibits significant deviation in certain parts from the predicted value, although once again the predicted is greater than the measured values. This effect is not of constant magnitude, as the test areas were at irregular intervals along the route, with a different road geometry at each point. To assess the effect of the

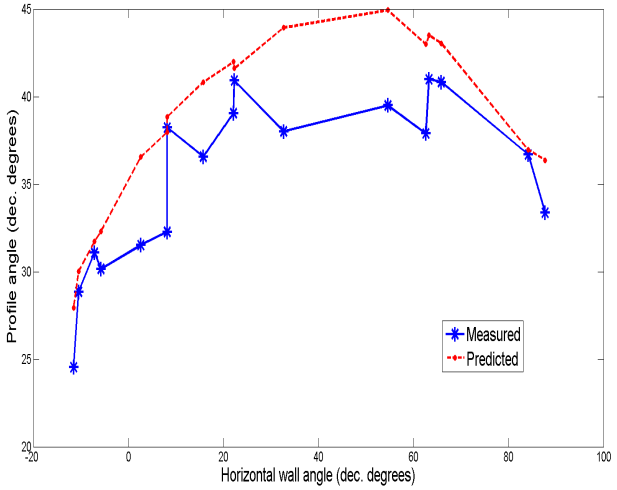

Figure 6: Profile angles for existing structures - Dataset 3

vehicle dynamics (specifically roll, pitch and yaw) on the profile angle, the measured profile data was compared to navigation data for each point.

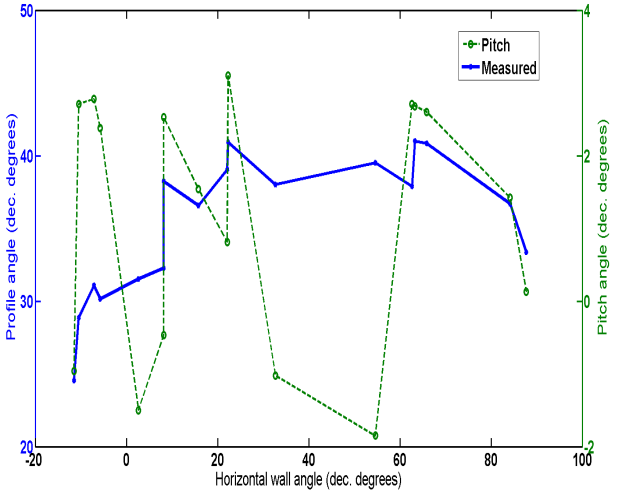

Figure 7: Measured angle and vehicle pitch - Dataset 3

To illustrate this effect, Figure 7 displays the effect of pitch on the profile angle. Changes in the angle of pitch occur at the points where the measured profile angle deviates from the predicted. Interestingly, when a large positive pitch angle is present, the measured profile angle comes closest to the predicted. When a negative pitch angle is apparent, the errors increase. Logically the predicted and measured should coincide closest to zero pitch. The cause of this is unclear, but appears to imply one or more of the following;

- The shock mounting holding the navigation sensors and laser scanner depresses slightly when the vehicle is in motion.
- Roll and pitch combined cause this effect.
- There is a difference in level in the MMS from the front to the rear (possibly physical, possibly due to acceleration).

There may be an as yet unidentified or unrecognised factor involved, it will require further study.

5 CONCLUSIONS AND FUTURE WORK

This study has taken our previous qualitative work on predicting profile angles for different mobile mapping systems on planar surfaces and incorporated a quantitative prediction method for dual axis scanner rotations on planar surfaces at any orientation. We have verified this method theoretically in a CAD environment and then experimentally using two real world datasets, one of a manufactured test route and one of existing features. Our system performed well in the CAD environment, and although errors were apparent in the real world tests, they appear to be linked to vehicle dynamics which can be compensated for. As yaw is unlikely to change significantly over the course of ten scan lines, once the angle of the wall to the direction of travel has been identified it can be ignored as a factor. Roll and pitch influence the profile angle, altering the surface normal of the scan plane and will have to be compensated for in the next iteration of our system. It is likely that by doing so it will minimise the errors significantly. One issue with this method is that this system is being designed to identify point density pre-mission, however roll and pitch will be unknowns at that time and so a minimum point density is likely be specified for objects on standard road gradients in our future work. It is hoped that this work will provide valuable information on MMS performance that can be used when defining future standards. Further work on point density will incorporate the navigation data to a greater extent and also point spacing on targets at different ranges.

ACKNOWLEDGEMENTS

The authors would like to acknowledge the support and funding received from the Irish Research Council for Science, Engineering and Technology (IRCSET) and the Enterprise Partner, Pavement Management Systems Ltd during this research.

The authors would also like to acknowledge assistance received from Dr. Stefan Bechtluft-Sachs from the NUI Maynooth Department of Mathematics and Statistics.

The LiDAR data framework presented in this paper was funded by the ERA-NET SR01 projects.

REFERENCES

Barber, D., Mills, J. and Smith-Voysey, S., 2008. Geometric validation of a ground-based mobile laser scanning system. ISPRS Journal of Photogrammetry and Remote Sensing 63(1), pp. 128–141.

Becker, S. and Haala, N., 2009. Grammar Supported Facade Reconstruction from Mobile LiDAR Mapping. International Archive of Photogrammetry and Remote Sensing XXXVIII Pa(2009), pp. 229–234.

Cahalane, C., McCarthy, T. and McElhinney, C., 2010a. Mobile mapping system performance - An initial investigation into the effect of vehicle speed on laser scan lines. In: Remote Sensing & Photogrammety Society Annual Conference - 'From the sea-bed to the cloudtops', September 2010, Cork, Ireland.

Cahalane, C., McElhinney, C. and McCarthy, T., 2010b. Mobile mapping system performance - an analysis of the effect of laser scanner configuration and vehicle velocity on scan profiles. In: European laser Mapping Forum - 'ELMF 2010', Novermber 2010, The Hague, Holland.

Goulette, F., Nashashibi, F., Abuhadrous, I., Ammoun, S. and Laurgeau, C., 2006. An integrated on-board laser range sensing system for on-the-way city and road modelling. In: Proceedings of the ISPRS Commission I Symposium,'From Sensors to Imagery', Vol. 61, Paris, France.

Graefe, G., 2007. Kinematic surveying with static accuracy. In: A. Grun and H. Kahmen (eds), 8th Conference on Optical 3-D Measurement Techniques, Zurich, Switzerland, pp. 142–149.

Haala, N., Peter, M., Kremer, J. and Hunter, G., 2008. Mobile LiDAR mapping for 3D point cloud collection in urban areas: a performance test. In: Proceedings of the 21st International Archives of the Photogrammetry, Remote Sensing and Spatial Information Sciences (ISPRS08, Vol. 37, Beijing, China, pp. 1119–1124.

Hammoudi, K., Dornaika, F. and Paparoditis, N., 2009. Extracting building footprints from 3d point clouds using terrestrial laser scanning at street level. International Archive of Photogrammetry and Remote Sensing XXXVIII Pa(2009), pp. 65–70.

Hesse, C. and Kutterer, H., 2007. A mobile mapping system using kinematic terrestrial laser scanning (KTLS) for image acquisition. In: A. Grun and H. Kahmen (eds), 8th Conference on Optical 3-D Measurement Techniques, Zurich, Switzerland, pp. 134–141.

Hofmann, S. and Brenner, C., 2009. Quality assessment of automatically generated feature maps for future driver assistance systems. In: Proceedings of the 17th ACM SIGSPATIAL International Conference on Advances in Geographic Information Systems - GIS '09, ACM Press, New York, New York, USA, pp. 500–503.

Kaartinen, H., Hyyppä, J., Gülch, E., Vosselman, G., Hyyppä, H., Matikainen, L., Hofmann, A. D., Mäder, U. and Persson, A., 2005. Accuracy of 3D City Models : EuroSDR comparison. In: International Archives of Photogrammetry, Remote Sensing and Spatial Information Sciences 36 (Part 3/W19), pp. 227–232.

Kukko, A., Andrei, C., Salminen, V., Kaartinen, H., Chen, Y., Rönnholm, P., Hyyppa, H., Hyyppa, J., Chen, R., Haggrén, H. and Others, 2007. Road Environment Mapping System of the Finnish Geodetic Institute-FGI Roamer. In: P. Ronnolm, H. Hyyppa and J. Hyyppa (eds), Proceedings of the ISPRS Workshop Laser Scanning 2007 and SilviLaser 2007, Espoo, Finland, 12-14 Sept. 2007, Vol. XXXVI, Espoo, Finland, pp. 241–247.

Kukko, A., Jaakkola, A., Lehtomaki, M., Kaartinen, H. and Chen, Y., 2009. Mobile mapping system and computing methods for modelling of road environment. In: 2009 Joint Urban Remote Sensing Event, Ieee, Shanghai, China.

Lehtomäki, M., Jaakkola, A., Hyyppä, J., Kukko, A. and Kaartinen, H., 2010. Detection of Vertical Pole-Like Objects in a Road Environment Using Vehicle-Based Laser Scanning Data. Remote Sensing 2(3), pp. 641–664.

Lewis, P., McElhinney, C., Schön, B. and Mccarthy, T., 2010. Mobile Mapping System LiDAR Data Framework. International Archives of the Photogrammetry, Remote Sensing and Spatial Information Sciences XXXVIII-4/W15, pp. 135–138.

Pu, S. and Vosselman, G., 2007. Extracting windows from terrestrial laser scanning. In: International Archives of Photogrammetry, Remote Sensing and Spatial Information Sciences Voll XXXVI, (Part 3/W52), Vol. 36number part 3, ISPRS, Espoo, Finland, pp. 320–325.

Riveiro, B., Armesto, J., Arias, P. and Gonza, H., 2011. Standard artifact for the geometric verification of terrestrial laser scanning systems. Optics Laser Technology.

Yoo, H., Goulette, F., Senpauroca, J. and Lepere, G., 2009. Simulation based comparative analysis for the design of laser terrestrial mobile mapping. In: Proceedings of the 6th International Symposium on Mobile Mapping Technology, Sao Paolo, Brazil., pp. 839–854.